



# Finite element investigation of the influence of a new transpedicular vertebral implant positioning on biomechanical responses of the spine segment

Ridha Hambli<sup>a,\*</sup>, Reade De Leacy<sup>b</sup>, François Cornelis<sup>c</sup>, Cécile Vienney<sup>d</sup>

<sup>a</sup> Univ. Orléans, Univ. Tours, INSA CVL, LaMé, 45000 Orléans, France

<sup>b</sup> Neurosurgery, Icahn School of Medicine at Mount Sinai, New York, NY, USA

<sup>c</sup> Memorial Sloan Kettering Cancer Center & Weill Cornell Medical College, Radiology Department, 1275 York Avenue, New York, NY 10065, USA

<sup>d</sup> Hyprevention, Research and Development, Pessac, France

## ARTICLE INFO

### Keywords:

Spine segment  
Compression fracture  
V-STRUT® device  
Positioning  
3D finite element

## ABSTRACT

The optimal positioning of an implant into a living organ such as femurs and vertebra is still an open problem. In particular, vertebral implant position has a significant impact on the results on spine behaviour after treatment in terms of stiffness, range of motion (ROM), wear, loosening and failure. In the current work, a 3D finite element analysis was conducted to investigate the positioning parameters of a novel transpedicular implant (V-STRUT®, Hyprevention, France) in terms of placement of the implant in the treated vertebra. The implant was designed in order to strength osteoporotic vertebral body and the related spine segment under compressive load. The effects of the axial and sagittal positions of the implant in the treated vertebra was investigated in terms of stress and stiffness variations.

A 3D finite element model of an osteoporotic spine segment was built based on a Computed Tomography (CT) scan of an osteoporotic female (69 yo). The model is composed of T12, L1 and L2 vertebrae and corresponding intervertebral discs and ligaments. The bone tissue was modeled as a heterogeneous material with properties assigned based on the grey scale levels. The intervertebral discs were modeled using two regions describing the annulus and the nucleus and linear beam elements with specific stiffness each were used representing each ligament.

The simulations indicated that the sagittal position (distance  $d$ ) plays a role on the stress distribution. The closer the implant to the interior wall the lower the stress applied to the spine segment. Nevertheless, the axial plane position (distance  $h$ ) have limited effects on the stress applied to the bone with a higher stress applied to the device (subjected to a higher bending load). These results can have direct clinical implications when dealing with the optimal placement of the implant. It is also possible to select a particular position in order to assign a given (target) stiffness for a patient.

## 1. Introduction

The occurrence of osteoporosis increases with aging leading to bone fragility increases.

Osteoporosis is characterized by low bone density associated with degeneration of bone microarchitecture and mechanical properties. Increasing the risk of vertebral compression fracture (VCF) is one of the main severe consequence of osteoporosis [1–3].

Several studies showed that about 30–50 % of women and 20–30 % of men will develop VCFs during their lives [3]. Approximately 25 % of

all postmenopausal women in the US have a VCF during their lifetime [4].

To enhance VCFs treatment, a novel device made of PEEK (polyetheretherketone) material (V-STRUT®) has been designed (Hyprevention, France) (Fig. 1-a). The device is composed of two cannulated implants that are introduced in the augmented vertebra across the pedicles followed by the injection of Polymethylmethacrylate (PMMA) cement. When the PMMA hardens, the implants are fixed and hence, strengthening the spine segment (Fig. 1-b). The device is indicated for use in the treatment of VCFs in the thoracic and lumbar spine from T9 to

\* Corresponding author at: Univ. Orléans, Univ. Tours, INSA CVL, LaMé, 8 rue Léonard de Vinci, 45000-Orléans, France.

E-mail address: [ridha.hamblil@univ-orleans.fr](mailto:ridha.hamblil@univ-orleans.fr) (R. Hambli).

<https://doi.org/10.1016/j.medengphy.2024.104100>

Received 10 May 2023; Received in revised form 7 November 2023; Accepted 1 January 2024

Available online 2 January 2024

1350-4533/© 2024 IPPEM. Published by Elsevier Ltd. All rights reserved.

L5 aimed to share axial loading between anterior and posterior columns and full vertebrae reinforcement [5,6]. In addition, the lateral hole of the implants ensure uniform cement distribution in the treated vertebral body.

The implant in combination with the injected cement was designed in order to strengthen osteoporotic vertebra and the related thoracolumbar spine.

Biomechanical behaviour restoration of a treated spine segment under compressive load is crucial to accomplish accurate function of the segment and durability of the implant.

Despite advances in surgical techniques, the effects of the positioning an implant into a vertebra must be investigated in order to optimise its position in term of biomechanical responses of the treated vertebra and related spine segment. It was reported that the position of the vertebral implants affects among others stress distribution and stiffness of the spine segment, reduced range of motion, wear of the implant [7–13] and failure load [14].

In addition, it was demonstrated that the lower is the applied stress on the implants; the higher is the applied stress on the bone [15]. These results may have implications in order to maintain the bone physiological value of applied peak strains in the bone. Frost, 2004 [26] showed that microstrain value applied to bone tissue must be in the range of (500–3000  $\mu\epsilon$ ) to maintain the bone organ in a healthy state and trigger the remodelling process. Thus, for a given device material and specific dimension, the implant position is a main factor impacting the treated spine segment biomechanical responses.

Gong et al. (2014) [13] performed a finite element study to investigate the biomechanical performance of a variety of pedicle screw fixation techniques. The authors concluded that placement and device variety have a strong impact on the biomechanical response of the spine. Pfeiffer et al. (2015) [14] investigated parameters that influenced failure of pedicle screw fixation in fusions and showed that placement of cement has significant influence on the failure load of the spine segment.

Probabilistic FE models developed by Rohlmann et al. (2013) [28] reported a strong relationship between the misalignment of vertebrae adjacent to a total disc replacement (TDR) and lumbar spine biomechanics.

It was reported that the position of a fixed-axis implant has strong influence of the range of motion [18] and that that optimal implant placement is patient-specific [28].

Hambli et al., (2023) [15] demonstrated that the treatment of VCFs fractures with the V-STRUT<sup>®</sup> device reduced the stress applied on the treated vertebrae and reestablished the stiffness of the related spine

segment. Nevertheless, there is still a concern that position of the device within the treated vertebra may play a role on the biomechanical responses of the spine segment.

Currently, bone cement augmentation techniques such as vertebroplasty and balloon kyphoplasty are the gold standards for surgical treatment of VCFs consisting in bone cement injection into the fractured vertebral body under pressure with the goal of stabilizing the fracture [5]. Such techniques have been shown to be effective treatment for VCFs. The novel V-STRUT technique combines cement injection and implant anchoring within the vertebra. When inserted in the bone organs, the cement plays a main role on the biomechanical performance of the augmented organs. Therefore, the purpose of the current preliminary study was to numerically investigate the effects of the position of the implant alone on the biomechanical responses of the vertebra and related spine segment. The bone cement was not considered in the present investigation with the goal to focus on the specific performance of the device.

## 2. Methods

A 3D finite element model of an osteoporotic spine segment was built based on a Computed Tomography (CT) scan of an osteoporotic female (69 yo) using the software ScanIP (Simpleware, Exeter, UK) (Fig. 3-a). The numerical model is composed of T12, L1 and L2 vertebrae and corresponding intervertebral discs. Two CAD implants geometries were imported and inserted in a second step in the middle of the treated vertebra along the pedicles (Fig. 3).

The effects of the axial and sagittal positions of the implant in the treated vertebra was investigated in terms of stress and stiffness variations.

The variables of the implant position are distance from anterior wall

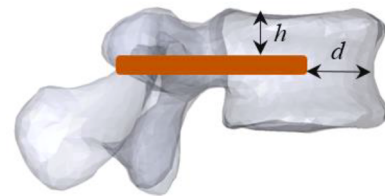
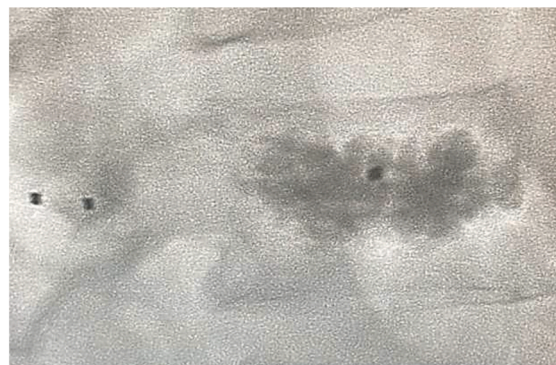


Fig. 2. Position factors of the V-STRUT<sup>®</sup> implant.  $d$ : distance from anterior wall,  $h$ : height from superior endplate.



(a)



(b)

Fig. 1. (a) CAD model Representing the V-STRUT<sup>®</sup> before cement injection. (b) A radiograph of a vertebral body treated with the V-STRUT<sup>®</sup> with bone cement injection.

(d) and height from superior endplate ( $h$ ) (Fig. 2).

The seven ligaments of the spine segment were considered in the current model as beam elements as reported by several studies [15, 21–23]. Depending on their locations and types (Fig. 3-d), linear beam elements were used in this work with varying stiffnesses representing the different ligaments (Fig. 3-d).

Five 3D Abaqus FE model was then generated for FE simulations (Fig. 3-d) to investigate the effect of the combination of clinical relevant  $d$  and  $h$  positions.

Model-1 (Reference): implant not inserted to be used as a reference results,

Model-2 (d5-h5): with inserted implant ( $d = 5$ ,  $h = 5$ ),

Model-3 (d5-h15): with inserted implant ( $d = 5$ ,  $h = 15$ ),

Model-4 (d15-h5): with inserted implant ( $d = 15$ ,  $h = 5$ ),

Model-5 (d15-h15): with inserted implant ( $d = 15$ ,  $h = 15$ ).

For each simulation, spine segment stiffness and stress distribution were computed and analyzed.

In Table 1 is reported the elements type and number of each spine segment component.

The characteristic length of the mesh size of about 0.7 mm was selected based on a mesh convergence studies performed using different mesh sizes (0.4 mm to 2.5 mm), which indicated that the chosen mesh resolution (0.7 mm) were not significantly less accurate than finer mesh.

The contact between vertebrae and discs and the facet joints was modelled using a Coulomb friction law with a friction coefficient value of 0.01 [15,16].

The implant was developed in order to strength osteoporotic vertebra and to prevent compressive fractures. Therefore, the load applied to the spine segment was limited to the axial compression with a pressure value of 1 MPa (case of climbing stairs) [17] applied to the upper surface of vertebra (T12) of about 1067 mm<sup>2</sup>. Reference node were added at the lower vertebra (L2) (Fig. 4-a) and the nodes at the end plate of the lower vertebra were fixed to the reference node. An encastre boundary condition where an encastewere then applied to the reference point [15].

The intervertebral discs were modeled using two regions (Fig. 4-b) describing the annulus and the nucleus, with the nucleus volume representing about approximately 40 % of the total disc area [18].

The heterogeneous Young modulus of the bone tissue is expressed by [19] as follows:

$$E = 15010\rho^{2.18} \quad (\rho \leq 0.280)$$

$$E = 6850\rho^{1.498} \quad (\rho > 0.280) \quad (1)$$

**Table 1**

Elements type and number of each model component.

Structure	Element type	Number
T12	Quadratic tetrahedral	431,200
L1	Quadratic tetrahedral	428,700
L2	Quadratic tetrahedral	429,350
T11-T12 disc	Quadratic tetrahedral	75,300
T12-L1 disc	Quadratic tetrahedral	74,800
L1-L2 disc	Quadratic tetrahedral	73,900
Ligaments	Linear beam elements	50 (for each ligament)
VSTRUT implant	Quadratic tetrahedral	67,900 (for each)

$\rho$  (g/cm<sup>3</sup>) denotes the bone density computed based on the CT values [19]:

Poisson's ratio of 0.3 was retained for the simulations.

A hyperelastic material model of type Mooney–Rivlin was applied for the intervertebral discs using a strain energy function given by [17,20]:

$$W = C10 (I_1 - 3) + C01 (I_2 - 3) \quad (2)$$

$I_1$  and  $I_2$  denotes the principal strain invariants and C01and C10are material properties.

Degenerated properties of intervertebral discs were retained (Table 2) in the present study [20].

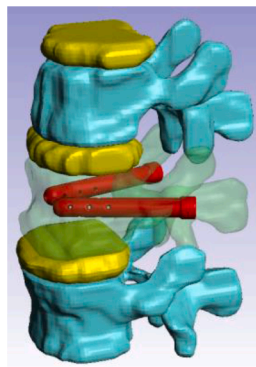
Spinal ligaments were modeled by linear elastic beam elements behavior with a specific stiffness value for each ligament (Table 3) reported from published literature [15,21–23].

The V-STRUT® implant is made of PEEK material which exhibits a linear isotropic behavior. Therefore in the current study, a Young modulus was set to  $E = 3600$  MPa and a Poisson ration set to  $\nu = 0.3$  [15, 24].

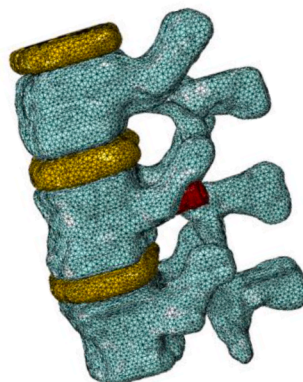
### 3. Results

Current model was validated by comparing the predicted stiffness of the non-treated spine segment (model 1) with previously published studies performed on different osteoporotic female spine segments (T12-L2) [25] (Table 4). In their investigation, the authors were destructively tested in axial compression twelve two functional spinal units (T6-T8, T9-T11, T12-L2 and L3-L5).

Predicted results (2206 N/mm) was in the range of the experimental one (2736 N/mm) reported in the study of Groenen et al. [25] for the case of an osteoporotic spine (segment: L12-T2) of a female. Despite the current investigated spine segment was different from the study of Groenen et al. [25], current prediction agrees well with the experimental one indicating that the proposed FE approach can be considered as being validated for compressive load.



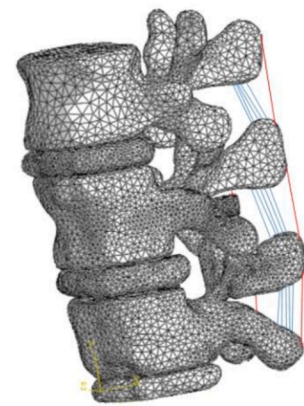
(a) Segmentation of the spine model



(b) FE meshing



(c) Detail of the implants



(d) FE model for simulations.

**Fig. 3.** 3D Finite element model built using three vertebrae, three intervertebral discs and ligaments.

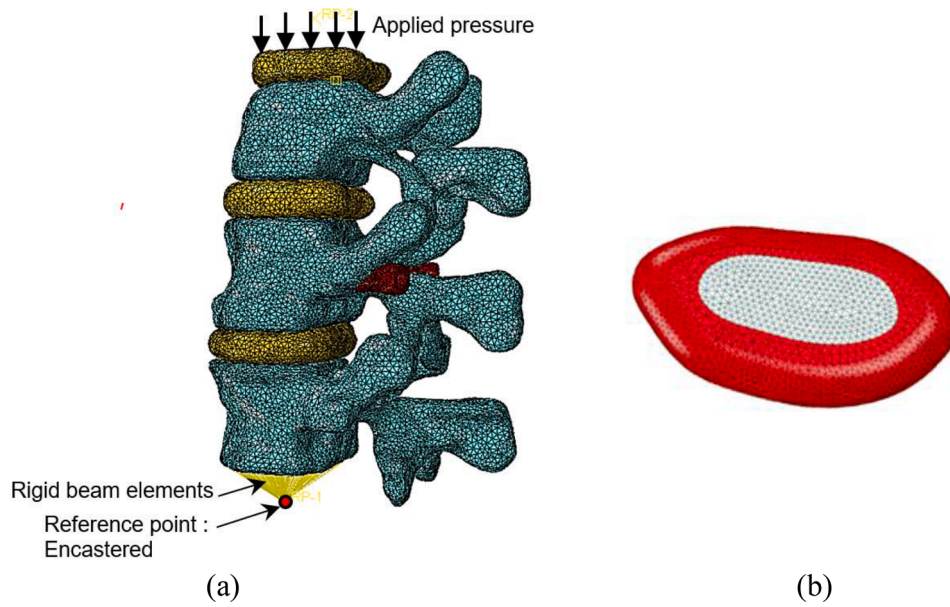


Fig. 4. (a) Boundary conditions. (b) Intervertebral disc partitioned into two volumes: Nucleus pulposus (light grey) and Annulus fibrosus (red).

**Table 2**  
Mooney–Rivlin material parameters of the intervertebral discs.

	$C_{01}$	$C_{10}$
Annulus	0.09	0.12
Nucleus	0.045	0.18

**Table 3**  
Ligament stiffnesses reported from [15,21–23].

Ligament	Stiffness (N/mm)
Longitudinal Anterior	210
Longitudinal Posterior	20.4
Supraspinale	23.7
Interspinale	11.5
Intertransversium	50
Flavum	27.2
Capsular	33.9

**Table 4**  
FE predicted values of stiffnesses for the different spine segment models.

Model	Stiffness (N/mm)	Difference in % compared to the reference model
Experiment [25]	2206	-
FE Reference (without implants)	2736	-
Model 1: d5-h5	3474	27 %
Model 2: d5-h15	3155	15.5 %
Model 3: d15-h5	3061	12 %
Model 4: d15-h15	2982	9 %

The effect of the implants positions in terms of stiffness variation can be observed in the Fig. 5. The stiffness of the reference model (without implants) is added for comparison.

It can be noticed that the placement of the implants (sagittal and axial planes) play a significant role on the spine segment rigidity. When the distance  $d$  increases, the stiffness decreases significantly when the device is placed in the middle (axial position:  $h = 15 \text{ mm}$ ) of the vertebra (Fig. 5-a). The distance  $h$  (axial position) plays also an important role when the device is fully inserted ( $d = 5 \text{ mm}$ ).

The computed von Mises stress contour in the model 1 (reference without implants) is depicted in Fig. 6.

The contour of the equivalent stress in the spine segment indicates that high stress occurs in the pedicles regions and in the middle of the vertebrae. It can be seen that the upper vertebra undergoes the highest value of the stress.

On Fig. 7 is plotted the stress distribution for two different implant positions from the anterior wall ( $d = 5 \text{ mm}$  and  $15 \text{ mm}$ ). The implant was placed at  $15 \text{ mm}$  from the superior endplate ( $h = 15 \text{ mm}$ ).

The results indicated that the stress level is lower when the implant is fully inserted in the vertebra ( $d = 5 \text{ mm}$ ) compared to a lower insertion level ( $d = 15 \text{ mm}$ ).

When comparing the effect of the implant position from the superior endplate, the FE simulations indicated that no noticeable stress variation exists in the vertebral body (Fig. 8). Nevertheless, a localized increase of the stress level can be observed in the pedicles region when the device is placed at  $5 \text{ mm}$  from the superior endplate ( $h = 5 \text{ mm}$ ).

The stress contour applied to the implants corresponding to the four models are plotted in Fig. 9.

The prediction demonstrated that depending on the device position, the stress peak value is ranging between  $5$  and  $10 \text{ MPa}$  and that the stress distribution was uniform applied on the implant region inserted in bone. The compressive load did generated stress concentration within involving compressive load dissipation. The combination of the implant design and the optimal selection of its placement showed an enhanced biomechanical behavior for the vertebra and the whole spine segment and for the integrity of the implant.

#### 4. Discussion and conclusions

Differences in the biomechanical behavior of treated osteoporotic spine with implants are not yet fully investigated in regard with the

$h$ (mm)	$d=5 \text{ mm}$	$d=15 \text{ mm}$	Without implants
5	3155	2982	2736
15	3474	3061	2736

Fig. 5. Variation of the predicted stiffness for different implant positions.

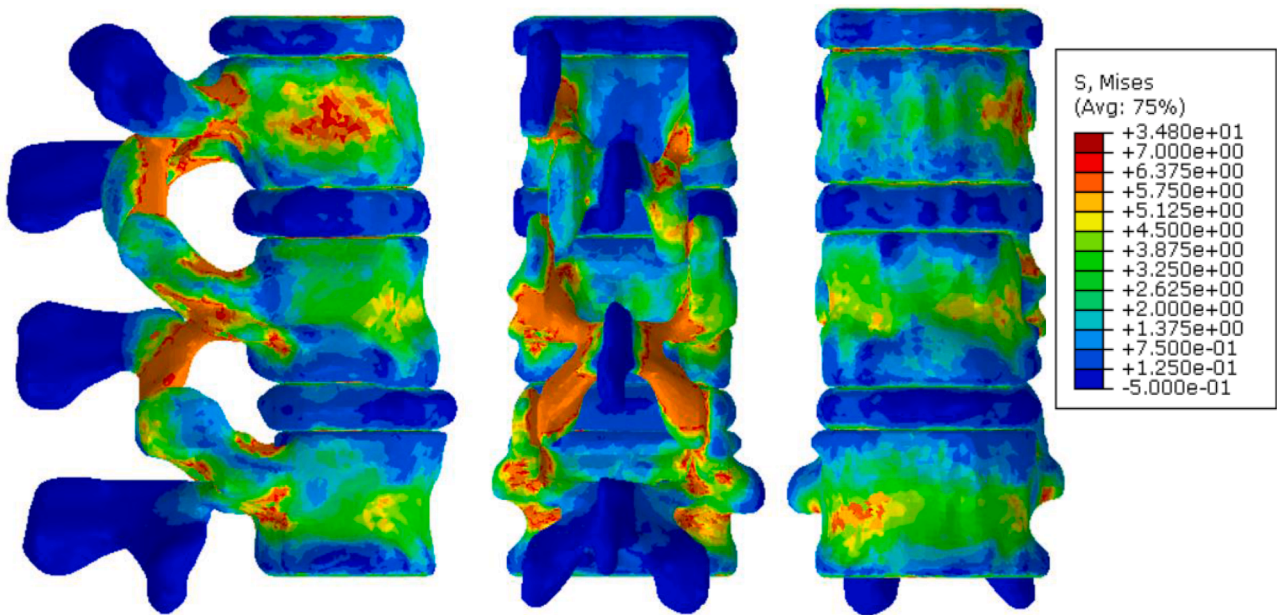
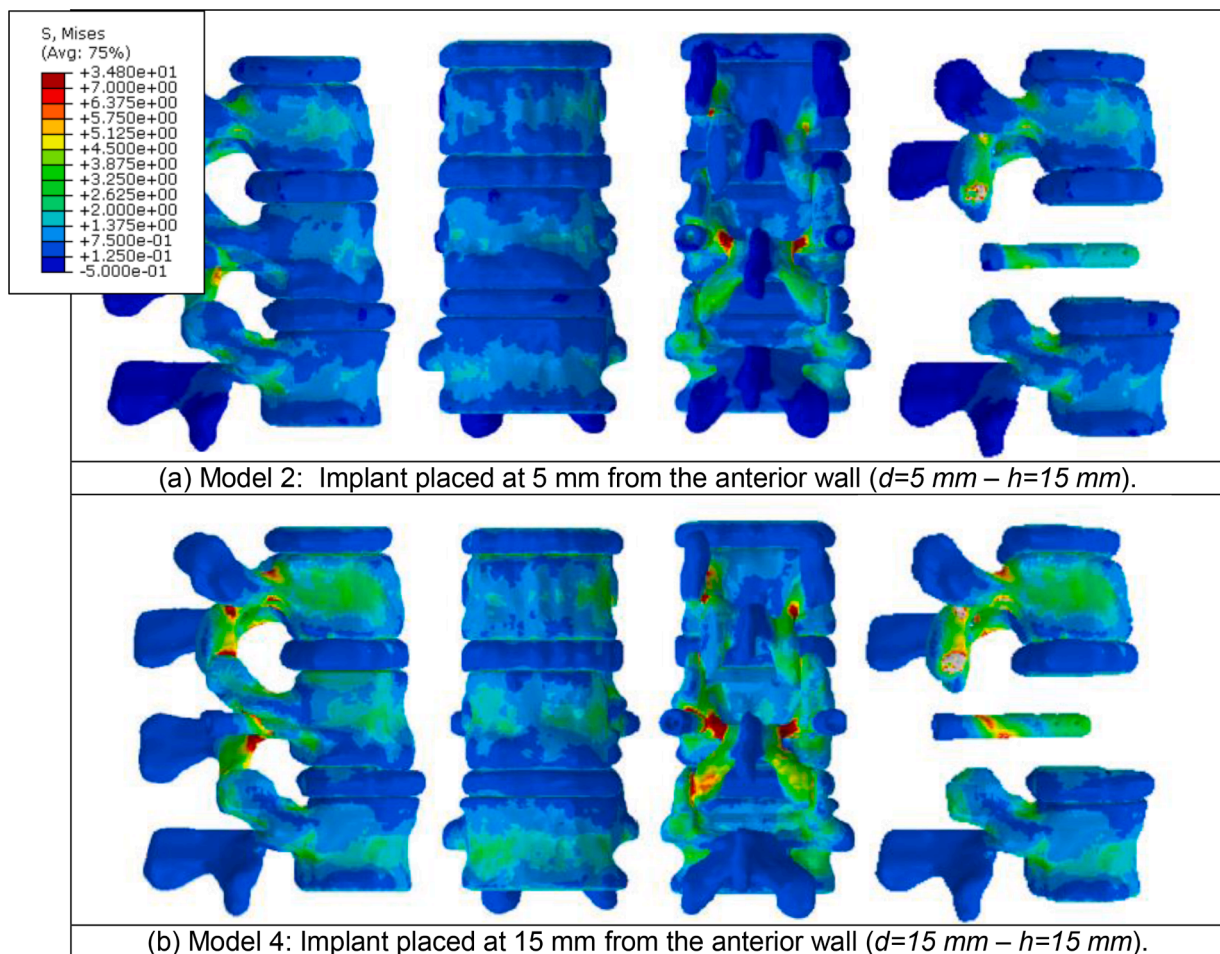


Fig. 6. von Mises stress contour in the spine segment (reference without implants).



(a) Model 2: Implant placed at 5 mm from the anterior wall ( $d=5\text{ mm} - h=15\text{ mm}$ ).

(b) Model 4: Implant placed at 15 mm from the anterior wall ( $d=15\text{ mm} - h=15\text{ mm}$ ).

Fig. 7. von Mises stress distribution within the spine segment. Models with two different positions of the implants from the anterior wall ( $d = 5\text{ mm}$  and  $15\text{ mm}$ ,  $h = 15\text{ mm}$ ).

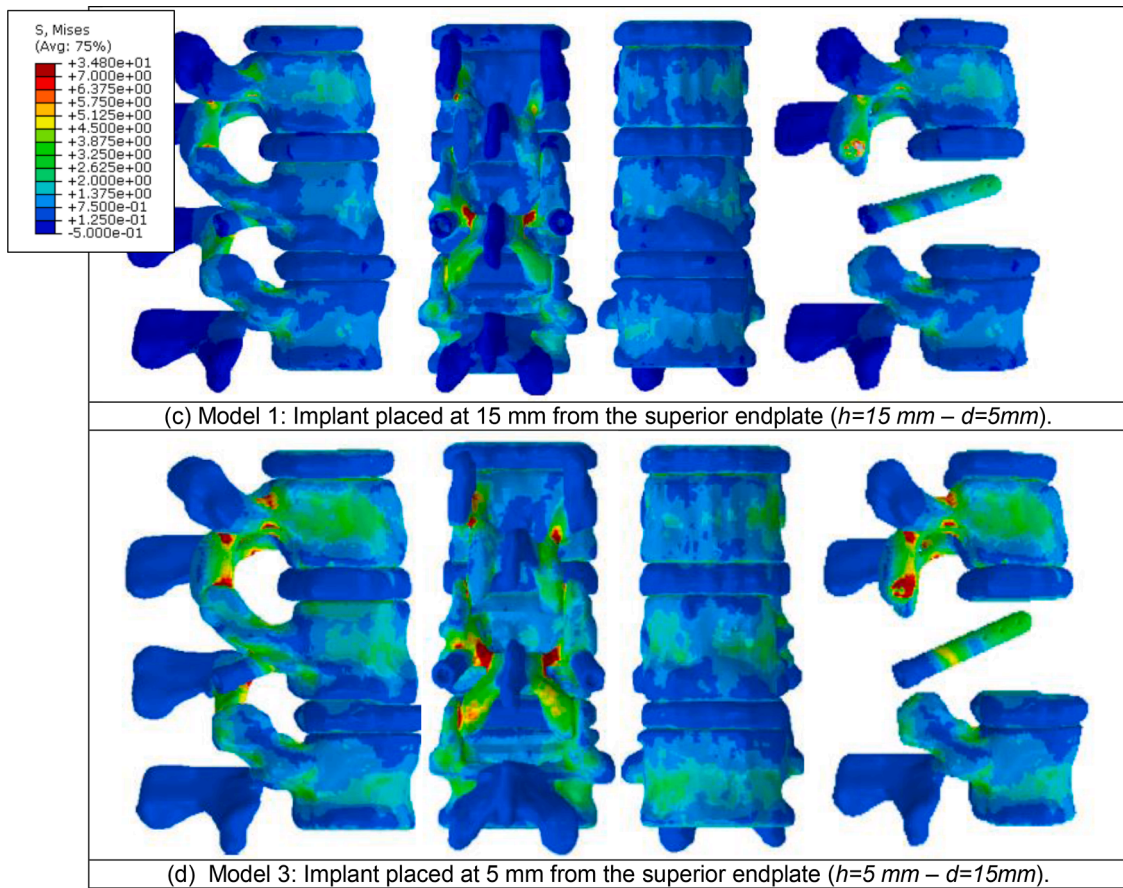


**Fig. 8.** von Mises stress distribution within the spine segment. Models with two different positions of the implants from the superior endplate ( $h = 5\text{ mm}$  and  $15\text{ mm}$ ,  $d = 5\text{ mm}$ ).

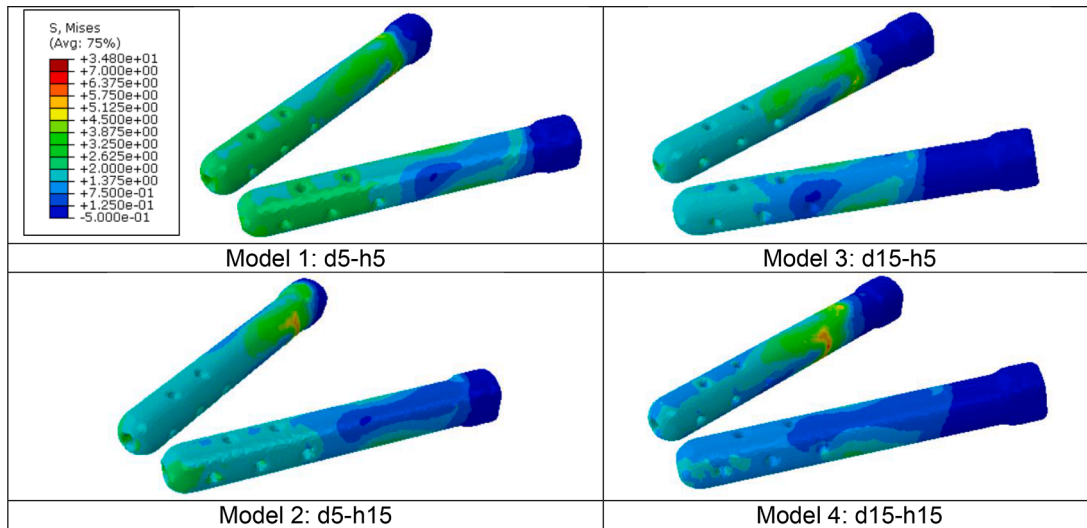


**Fig. 9.** Stress distribution applied to the implants.

implant position. In the current study, five 3D FE model were developed of a lumbar spine segment with different positions of the V-STRUT® device representing clinical possibly placement of the implants.

The implant aims to reduce stress applied to the treated vertebral body, to reestablished vertebral resistance, stabilize and prevent the progression of postoperative fractures under compressive load by sharing the axial compressive loading between anterior and posterior columns. Therefore, when evaluating the biomechanical effects of the

device positioning, the impact of the different insertion positions should be investigated. Finite element analysis allowed us to understand how spine segment stiffness and stress distribution in vertebral body and in V-STRUT® device can be influenced by the implant position within a treated vertebra. The V-STRUT® device made of PEEK placed at different positions presented different mechanical response of bone and implants in simulating compressive load applied to a spine segment.

Plots of Fig. 9 showed that the best position of the implant allowing a

uniform stress distribution in the implant region inserted in the vertebral body correspond to the model 2 (d5-h15). This result has significant implication when considering the long-term biomechanical effects of the augmented vertebra. It is well known that rigid implants stabilize the bone organ. Nevertheless, high stiffness behavior of the implant may generate the phenomenon of stress shielding resulting in bone loss at bone region located around the bone/implant interface [27].

When comparing the stiffness of the spine segment with and without implantation of the device (Table 3), our results indicated that the mean percentage increases with respect to the reference model (without implants) ranged between +9 % and +35 % depending on the implants positions.

It can be noticed that the placement of the implants play a significant role on the spine segment rigidity. When the distance from the anterior wall ( $d$ ) decreases the stiffness increases to reach its maximum value. For a reduced distance (the implant is inserted about 50 %), the stiffness is lower compared to the fully inserted configuration but higher to the stiffness of the reference model (without implants). These stiffnesses variation were modulated by the implant height from superior endplate. The placement of the implant in the middle height (about  $h = 15 \text{ mm}$ ) predicted an increase of the stiffness in combination with the position from the interior wall.

The whole simulation predicted that the best position generating the maximum stiffness increase correspond to a full insertion of the implant ( $d = 5 \text{ mm}$ ) in the middle of the axial plane of the treated vertebra ( $h = 15 \text{ mm}$ ). These results can have direct clinical implications when dealing with the optimal placement of the implant. It is also possible to select a particular position in order to assign a given (target) stiffness for a patient.

A main clinical concern in relation with the implant position within bone organ is to generate an optimal restoration of the stress distribution and the strength of the augmented bone. Rohlmann et al., 2013 [28] performed a FE study to investigate the performance of different spine-stabilizing implants and showed that significant stress and stiffness variations applied on the augmented vertebra and spine segment exists when comparing the different implants and related positions.

Results of Fig. 8 indicated that when the implant is placed close to the endplate ( $h = 5 \text{ mm}$ ), a part of the stress is transferred mainly to the superior adjacent vertebra. The placement of the implant close to the superior endplate reinforced the augmented vertebral stiffness and hence, played a role as a barrier for stress transfer to the upper vertebra. Therefore, this can reduced the cushioning capability of the augmented vertebra and increase of the stress to the upper adjacent one. In addition, placement of the implant close to the superior endplate may alter the natural inward bulging of the endplate and increase the pressure on the adjacent discs.

In another side, it was reported that cement leakage is a significant risk factor generating adjacent vertebral fractures [29]. Such a leakage may generate significant change in the biomechanical response of the augmented vertebra and related spine segment combined with the osteoporosis progression [30,31]. From a clinical point of view, the placement of the implant in relation with its position and geometry suggests that the closer the implant position to the anterior wall (low value of distance  $d$ ) and to the superior endplate (low value of distance  $h$ ), higher the risk of cement leakage. In addition, the implant is inserted through the pedicle. The other cannulated part of the implant is placed in the vertebral body. These lateral holes ensure a controlled cement diffusion into the augmented vertebra with a low cement of pressure amplitude. Hence, lowering the risk of cement leakage.

The current study enhances the understanding of the role of the positioning of the new implant biomechanical effects on a treated spine segment. The FE simulations indicated that optimal device position play a significant role in order to assign a given spine segment stiffness and stress distribution in order to restore the spine with the goal to the reduce the risk of in the adjacent vertebral fractures.

Despite the rational construction of the present FE model, present study has some limitations. First, the geometrical model is limited to a non-fractured one female patient. Additional studies with a larger population are required to study the biomechanical behaviour of the V-STRUT® device for different spine models. In addition, personalized simulations are required to study the effects of the performance of the device. The second limitation concerns the modelling of the cement effects in combination with the implant.

In the present investigation, the specific objective was to investigate the performance of the device alone under compressive load in relation with its position within the augmented vertebra and the spine segment. Our FE model focused on the role of the implant alone. And addressed only the behaviour under compressive load. However, *In vivo* loading of the spine includes combination of different mechanical loading such as torsion, bending, flexion, and extension and different doses of cement. However, the device was designed mainly to restore vertebral compressive fractures. Therefore, the compressive load case retained in the current work was considered sufficient to investigate the role of the implant position. Nevertheless, additional investigations are required to study the biomechanical performance of the V-STRUT® device in combination with different doses of cement under different loading modes.

Within the limitations of this study, FE simulations have revealed that the sagittal and axial positions of the V-STRUT® device affects the biomechanical response of the treated vertebra, related spine segment and the device in terms of stiffness and applied stress.

In conclusion, obtained results using the 3D FE model indicated clearly that the position of the novel transpedicular device (V-STRUT®, Hyprevention, France) plays a significant role on the biomechanical response of an augmented vertebra in terms of stress distribution and spine segment stiffness. From a clinical point of view, this study has confirmed the general conclusion that varying the position of a vertebral body device can modulate the spine segment strength and stiffness that play an important role of the patients' outcomes. In addition, it is possible to select an optimal position of the implants in order to optimize the augmented spine segment stiffness to develop better personalized strategies to reduce VCFs.

## Funding

None.

## Ethical approval

Not required.

## Declaration of competing interest

The study was sponsored by Hyprevention. None declared.

## Acknowledgement

MSKCC is funded through the NIH/NCI Cancer Center Support Grant P30 CA008748.

## References

- [1] Melton III LJ. Epidemiology of spinal osteoporosis. *Spine* 1997;22(24):2S–11S. suppl.
- [2] Balasubramanian A, Zhang J, Chen L, Wenkert D, Daigle SG, Grauer A, Curtis JR. Risk of subsequent fracture after prior fracture among older women. *Osteoporos Int* 2019;30:79–92.
- [3] Ross PD. Clinical consequences of vertebral fractures. *Am J Med*:103: 30S42S; discussion 1997:42S–3S.
- [4] Wong Cyrus C, McGirt Matthew J. Vertebral compression fractures: a review of current management and multimodal therapy. *J Multidiscip Healthc* 2013;6: 205–14.

- [5] Aebi M, Maas C, Di Pauli von Treuheim T, Friedrich H, Wilke HJ. Comparative biomechanical study of a new transpedicular vertebral device and vertebroplasty for the treatment or prevention of vertebral compression fractures. *Clin Biomech* 2018;56:40–5.
- [6] Cornelis FH, Barral M, Le Huec JC, Deschamps F, De Baere T, Tselikas L. Percutaneous transpedicular fixation by PEEK polymer implants combined with cementoplasty for vertebral compression fractures: a pilot study. *Cardiovasc Intervent Radiol* 2021;44(4):642–6.
- [7] Bellato RT, Teixeira WGJ, Torelli AG, Cristante AF, de Barros TEP, de Camargo OP. Late failure of posterior fixation without bone fusion for vertebral metastases. *Acta Ortopedica Brasileira* 2015;23:303–6.
- [8] Glorion M, Dubory A, Mitilian D, Gomez-Caro A, Darteville P, Court C, Fadel E, Misenard G. Long-term mechanical results of partial thoracic vertebrectomies with posterior instrumentation only after en bloc tumoral resection. *Eur Spine J* 2016; 25:2339–40.
- [9] Pedreira R, Abu-Bonsrah N, Karim Ahmed A, De la Garza-Ramos R, Rory Goodwin C, Gokaslan ZL, Sacks J, Sciubba DM. Hardware failure in patients with metastatic cancer to the spine. *J Clin Neurosci* 2017;45:166–71.
- [10] Shimura K, Kato S, Demura S, Yokogawa N, Yonezawa N, Shimizu T, Oku N, Kitagawa R, Handa M, Anzen R, Murakami H, Tsuchiya H. Revision surgery for instrumentation failure after total en bloc spondylectomy: a retrospective case series. *BMC Musculoskelet Disord* 2020;21:66.
- [11] Wong YC, Chau WWJ, Kwok KO, Law SW. Incidence and risk factors for implant failure in spinal metastasis surgery. *Asian Spine J* 2020;14:878–85.
- [12] Yoshioka K, Murakami H, Demura S, Kato S, Yokogawa N, Kawahara N, Tomita K, Tsuchiya H. Risk factors of instrumentation failure after multilevel total en bloc spondylectomy. *Spine Surg Rel Res* 2017;1:31–9.
- [13] Gong Z, Chen Z, Feng Z, Cao Y, Jiang C, Jiang X. Finite element analysis of 3 posterior fixation techniques in the lumbar spine. *Orthopedics* 2014;37(5):e441–8.
- [14] Pfeiffer FM, Choma TJ, Kueny R. Finite element analysis of Stryker Xia pedicle screw in artificial bone samples with and without supplemental cement augmentation. *Comput Methods Biomech Biomed Eng* 2015;18(13):1459–67.
- [15] Hambli R, De Leacy R, Vienney C. Effect of a new transpedicular vertebral device for the treatment or prevention of vertebral compression fractures: a finite element study. *Clin Biom* 2023;(102):105893.
- [16] Wan S, Xue B, Xiong Y. Three-dimensional biomechanical finite element analysis of lumbar disc herniation in middle aged and elderly. *J Healthc Eng* 2022;15: 7107702. 2022.
- [17] Wilke H J, Neef P, Caimi M, Hoogland T, Claes L E. New in vivo measurements of pressures in the intervertebral disc in daily life. *Spine (Phila Pa 1976)* 1999;24(8): 755–62. 15.
- [18] Dreischarf M, Zander T, Shirazi-Adl A, Puttlitz CM, Adam CJ, Chen CS, Goel VK, Kiapour A, Kim YH, Labus KM, Little JP, Park WM, Wang YH, Wilke HJ, Rohlmann A, Schmidt H. Comparison of eight published static finite element models of the intact lumbar spine: predictive power of models improves when combined together. *J Biomech* 2014;47:1757–66.
- [19] Morgan EF, Bayraktar HH, Keaveny TM. Trabecular bone modulus-density relationships depend on anatomic site. *J Biomech* 2003;36(7):897–904.
- [20] Schmidt H, Heuer F, Drumm J, Klezl Z, Claes L, Wilke HJ. Application of a calibration method provides more realistic results for a finite element model of a lumbar spinal segment. *Clin Biomech* 2007;22:377–84.
- [21] Pintar FA, Yoganandan N, Myers T, Elhagediab A, Sances Jr A. Biomechanical properties of human lumbar spine ligaments. *J Biomech* 1992;25:1351–6.
- [22] Neumann P, Keller TS, Ekström L, Hansson T. Effect of strain rate and bone mineral on the structural properties of the human anterior longitudinal ligament. *Spine* 1994;19:205–11.
- [23] Polikeit A, Nolte LP, Ferguson SJ. The effect of cement augmentation on the load transfer in an osteoporotic functional spinal unit: finite-element analysis. *Spine* 2003;28:991–6.
- [24] Jhong GH, Chung YH, Li CT, Che YN, Chang CW, Chang CH. Numerical comparison of restored vertebral body height after incomplete burst fracture of the lumbar spine. *J Pers Med* 2022;12(2):253. 10.
- [25] Groenen KHJ, Bitter T, Veluwen TCG, van der Linden YM, Verdonschot N, Tanck E, Janssen D. Case-specific non-linear finite element models to predict failure behavior in two functional spinal units. *J Orthop Res* 2018;36(12):3208–18.
- [26] Frost HMA. A 2003 update of bone physiology and Wolff's Law for clinicians. *Angle Orthod* 2004;74(01):3–15.
- [27] Jamari J, Ammarullah MI, Santoso G, Sugiharto S, Supriyono T, Prakoso AT, Basri H, van der Heide E. Computational contact pressure prediction of CoCrMo, SS 316L and Ti6Al4V femoral head against UHMWPE acetabular cup under gait cycle. *J Funct Biomater* 2022;13:64.
- [28] Rohlmann A, Lauterborn S, Dreischarf M, Schmidt H, Putzier M, Strube P, Zander T. Parameters influencing the outcome after total disc replacement at the lumbosacral junction. Part 1: misalignment of the vertebrae adjacent to a total disc replacement affects the facet joint and facet capsule forces in a probabilistic finite element analysis. *Eur Spine J* 2013;22(10):2271–8.
- [29] Lin EP, Ekholm S, Hiwatashi A, Westesson PL. Vertebroplasty: cement leakage into the disc increases the risk of new fracture of adjacent vertebral body. *AJNR Am J Neuroradiol* 2004;25:175–80.
- [30] Noriega D, Marcia S, Theumann N, Blondel B, Simon A, Hassel F, Maestretti G, Petit A, Weidle PA, Mandly AG, Kaya JM, Touta A, Fuentes S, Pflugmacher R. A prospective, international, randomized, noninferiority study comparing an implantable titanium vertebral augmentation device versus balloon kyphoplasty in the reduction of vertebral compression fractures (SAKOS study). *Spine J* 2019;19 (11):1782–95.
- [31] Han S, Jang IT. Analysis of adjacent fractures after two-level percutaneous vertebroplasty: is the intervening vertebral body prone to te-fracture? *Asian Spine J* 2018;12:524–32.